# Solubilities of lanthanum oxide in fluoride melts
# Part I. Solubility in $M_3AlF_6$ (M = Li, Na, K)

M. Ambrová [*], J. Jurišová

*Department of Inorganic Technology, Faculty of Chemical and Food Technology, Slovak University of Technology, SK-81237 Bratislava, Slovakia*

## Abstract

Solubility of lanthanum oxide was measured by thermal analysis. The solubility in alkali cryolites is rather high, because of chemical reactions between lanthanum oxide and cryolites. In $Li_3AlF_6$–$La_2O_3$, alumina precipitates, in the other systems the mixed oxide $LaAlO_3$ is formed. In $La_2O_3$–$Li_3AlF_6$ the eutectic point is at 9.5 mol% $La_2O_3$ and 755 °C. The eutectic points in $La_2O_3$–$Na_3AlF_6$ and $La_2O_3$–$K_3AlF_6$ are at 11.5 mol% $La_2O_3$, and at 937 and 934 °C, respectively.
© 2006 Elsevier B.V. All rights reserved.

*Keywords:* Solubility; Lanthanum oxide; Molten cryolite; Molten fluorides; Thermal analysis

## 1. Introduction

There is wide interest in reprocessing of spent nuclear fuel. A promising way of reprocessing is the use of molten salts and particularly fluoride melts. The advantages are their solvent properties for the dissolution of the fuel; they have a large electrochemical window and are not sensitive to radiolytic degradation [1,2]. This work is a part of a project dealing with electroseparation of the constituents of spent MOX fuel. Lanthanum compounds in fluoride melts were chosen as a model system. This paper deals with solubility and phase diagrams of lanthanum oxide–alkali cryolite melts. No data on solubility or phase diagrams of the systems are available.

## 2. Experimental

The temperatures of phase transitions were determined by thermal analysis, recording the cooling and heating curves of mixtures at 2–5 °C/min in a resistance furnace with an adjustable cooling rate. A platinum crucible containing 30 g of sample was placed into the furnace pre-heated to the temperature of fusion of pure alkali cryolite. (At the compositions where crystallization of $La_2O_3$ was expected, the temperature was higher.) The sample

was kept 1 h at the temperature and regularly stirred by platinum wire. The sample was slowly cooled after that time. Temperature was measured with a PtRh10-Pt thermocouple calibrated to the melting points of NaF, $BaCl_2$, NaCl, KCl, LiF and $Na_2SO_4$. The measured transition temperatures were reproducible within ±2 °C.

The following chemicals were used: LiF, NaF (Lachema, analytical grade), $AlF_3$, KF, $La_2O_3$ (Mikrochem, pure) and $P_2O_5$ (Mikrochem, analytical grade). LiF, NaF and $La_2O_3$ were dried at 600 °C for 2 h, KF was dried in a vacuum drying oven in the presence of $P_2O_5$ and $AlF_3$ was purified by sublimation.

The samples were analysed by X-ray diffraction (STOE automated theta/theta diffractometer, Germany, Co K$\alpha_1$ radiation, $\lambda = 0.17902$ nm) from 5° to 80° 2$\theta$. The positions of the basal reflections were determined by Bede ZDS program.

## 3. Theoretical

Thermodynamic models of systems containing complex compounds are usually based on the assumption of partial dissociation of the compounds [3]. However, the structure of cryolite-based melts is not reliably known [4]. The model presented below is independent of the structure of the melt. The model is described in detail by Danielik et al. [5–7]. It assumes the ideal melt contains only ionic pairs of the basic species. In the case of the complex compounds in the solid phase, the compounds are assumed to completely dissociate to the basic species.

---
[*] Corresponding author.
*E-mail address:* marta.ambrova@stuba.sk (M. Ambrová).

Table 1
Coefficients of the excess Gibbs energy of the systems $La_2O_3$–$M_3AlF_6$ (M = Li, Na, K) according to Eqs. (5) and (8)

| System | Coefficient (J mol$^{-1}$) | Reference |
|---|---|---|
| LiF–LiAlF$_4$–La$_2$O$_3$ | $g_0 = -(144.6 \pm 3.5) \times 10^3 + T \times (106 \pm 7)$ | [8,9] |
| | $g_1 = (183.7 \pm 13.0) \times 10^3 - T \times (147 \pm 16)$ | [8,9] |
| | $g_2 = -(87.4 \pm 11.6) \times 10^3 + T \times (75 \pm 14)$ | [8,9] |
| | $g_3 = 0$ | [8,9] |
| | $g_{111} = 0$ | This work |
| NaF–NaAlF$_4$–La$_2$O$_3$ | $g_0 = -(95.6 \pm 3.5) \times 10^3 + T \times (44 \pm 1)$ | [10,11] |
| | $g_1 = -(249.3 \pm 25.4) \times 10^3 + T \times (202 \pm 3)$ | [10,11] |
| | $g_2 = (659.1 \pm 57.5) \times 10^3 - T \times (502 \pm 7)$ | [10,11] |
| | $g_3 = -(457.4 \pm 40.4) \times 10^3 + T \times (348 \pm 5)$ | [10,11] |
| | $g_{111} = -(173.2 \pm 11.0) \times 10^3$ | This work |
| KF–KAlF$_4$–La$_2$O$_3$ | $g_0 = -(66.7 \pm 5.3) \times 10^3 + T \times (14 \pm 4)$ | [7] |
| | $g_1 = -(227.6 \pm 40.3) \times 10^3 + T \times (200 \pm 22)$ | [7] |
| | $g_2 = (426.2 \pm 90.0) \times 10^3 - T \times (331 \pm 53)$ | [7] |
| | $g_3 = -(190.8 \pm 60.2) \times 10^3 + T \times (138 \pm 46)$ | [7] |
| | $g_{111} = -(159.5 \pm 14.7) \times 10^3$ | This work |

$T$ is temperature in Kelvin.

Consider the system AX–BX, in which a compound $(AX)_p \cdot (BX)_q$ exists in the solid state. The activities of AX and BX are (standard state corresponds to pure component at the temperature and pressure of the melt)

$$a(AX) = x(AX) \cdot \gamma(AX), \qquad a(BX) = x(BX) \cdot \gamma(BX) \qquad (1)$$

Activity coefficients of AX and BX can be obtained from the molar excess Gibbs energy

$$RT \ln \gamma_i = \left[ \frac{\partial (\sum n_i \, \Delta G_i^E)}{\partial n_i} \right]_{T, p, n_{j \neq i}} \qquad (2)$$

If we assume that the chemical potential of the compound $(AX)_p \cdot (BX)_q$ corresponding to its standard state is

$$\mu[(AX)_p \cdot (BX)_q] = p\mu(AX) + q\mu(BX) \qquad (3)$$

then for the activity of $(AX)_p \cdot (BX)_q$ [5–7]

$$\begin{aligned} a[(AX)_p(BX)_q] &= x[(AX)_p(BX)_q] \cdot \gamma[(AX)_p(BX)_q] \\ &= \frac{x(AX)^p \cdot x(BX)^q}{x(AX)_0^p \cdot x(BX)_0^q} \cdot \frac{\gamma(AX)^p \cdot \gamma(BX)^q}{\gamma(AX)_0^p \cdot \gamma(BX)_0^q} \end{aligned} \qquad (4)$$

where $x(i)_0$ and $\gamma(i)_0$ are the mole fractions and activity coefficients of AX and BX in the melt with the composition of the pure compound $(AX)_p \cdot (BX)_q$, respectively.

In the binary system the composition dependence of the molar excess Gibbs energy can be described by

$$\Delta G_m^E = x_1 x_2 (g_0 + g_1 x_2 + g_2 x_2^2 + g_3 x_2^3) \qquad (5)$$

When data on the enthalpy of mixing are available, we can express the molar excess Gibbs energy from the classical relationship

$$\Delta G_m^E = \Delta H_{m,mix} - T \, \Delta S_m^E \qquad (6)$$

where $\Delta H_{m,mix}$ and $\Delta S_m^E$ are assumed to be independent of temperature and may be described by similar equations as Eq. (5).

The molar excess Gibbs energy of the ternary system can be described by the relationship

$$\Delta G_m^E = \sum \Delta G_{m, \, binary}^E + \sum g_{ijk} x_1^i x_2^j x_3^k \qquad (7)$$

where $i$, $j$ and $k$ are integer values.

The cryolite $M_3AlF_6$ is a part of the system $MF$–$AlF_3$. Because no free $AlF_3$ exists in these systems, the system $MF$–$MAlF_4$ is more appropriate for description of the systems. Thus, the system $M_3AlF_6$–$La_2O_3$ can be described as a part of the system $MF$–$MAlF_4$–$La_2O_3$. The temperature dependencies of the excess Gibbs energy of the binary systems $MF$–$MAlF_4$ were presented in [7–11]. The coefficients of Eq. (5) of the system are in Table 1. The excess Gibbs energy of the ternary system $MF$–$MAlF_4$–$La_2O_3$ can be described by Eq. (7). However, the other binary systems are not known. Therefore, it was assumed that the binary systems $MF$–$La_2O_3$ and $MAlF_4$–$La_2O_3$ are almost ideal. It follows from calculated data that the excess Gibbs energy of the systems $MF$–$MAlF_4$–$La_2O_3$ can be described as

$$\Delta G_m^E = \Delta G_m^E(MF\text{–}MAlF_4) + g_{111}x(MF)x(MAlF_4)x(La_2O_3). \qquad (8)$$

## 4. Results and discussion

### 4.1. System Li$_3$AlF$_6$–La$_2$O$_3$

The liquidus temperatures in the system $Li_3AlF_6$–$La_2O_3$ were measured up to 11 mol% $La_2O_3$. The measured and calculated part of the phase diagram is shown in Fig. 1. The standard deviation of the calculated data was $\sigma = 1.55\,°C$. The coordinates of eutectic point are 9.5 mol% $La_2O_3$ and 755 °C.

The sample 10 mol% $La_2O_3 + 90$ mol% $Li_3AlF_6$ was quenched and X-ray diffraction analysis made at room temperature. At the bottom of the sample there were small lumps of pure alumina. The rest of the sample contained LiF, LaF$_3$
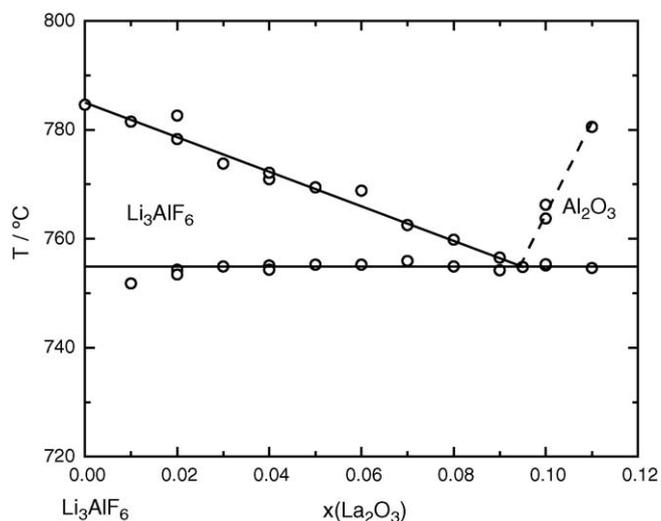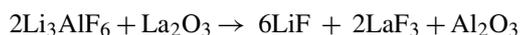
Fig. 1. Phase diagram of the system $Li_3AlF_6$–$La_2O_3$. (◯) Experimental; (—) calculated.

and $Al_2O_3$ (Fig. 2). It seems that the following reaction occurs:

$$2Li_3AlF_6 + La_2O_3 \rightarrow 6LiF + 2LaF_3 + Al_2O_3$$

From the formation of lumps of alumina one may conclude that the alumina is the first crystallizing phase at the measured composition.

### 4.2. System $Na_3AlF_6$–$La_2O_3$

The transition temperatures in the system $Na_3AlF_6$–$La_2O_3$ were measured up to 13 mol% $La_2O_3$. The measured and calculated part of the phase diagram is shown in Fig. 3.

The standard deviation of the calculated data was $\sigma = 2.15\,°C$. The coordinates of eutectic point are 11.5 mol% $La_2O_3$ and 937 °C.

The sample 10 mol% $La_2O_3$ + 90 mol% $Na_3AlF_6$ was quenched and X-ray diffraction analysis was made at the room temperature. It can be seen from Fig. 4 that the sample has contained NaF, $Na_3AlF_6$, $NaLaF_4$ and $LaAlO_3$. It seems that
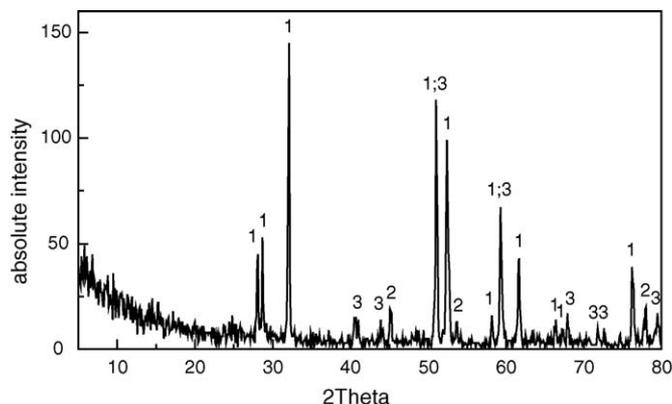


Fig. 2. X-ray record of the frozen melt of the system $Li_3AlF_6$–$La_2O_3$ (10 mol% of $La_2O_3$). (1) $LaF_3$; (2) LiF; (3) $Al_2O_3$.
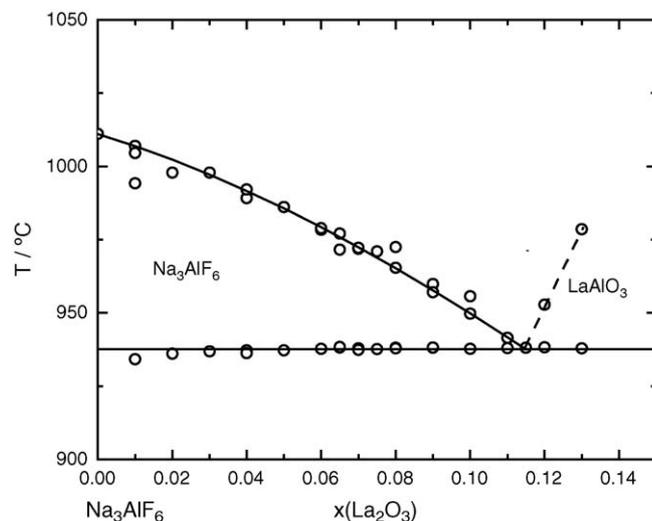


Fig. 3. Phase diagram of the system $Na_3AlF_6$–$La_2O_3$. (◯) Experimental; (—) calculated.

following reaction takes part in the system:

$$Na_3AlF_6 + La_2O_3 \rightarrow 2NaF + NaLaF_4 + LaAlO_3$$

Thus, it may be concluded that $LaAlO_3$ is the first crystallizing phase at the measured composition.

### 4.3. System $K_3AlF_6$–$La_2O_3$

The temperatures of the primary crystallization in the system $K_3AlF_6$–$La_2O_3$ were measured up to 13 mol% $La_2O_3$. The measured and calculated part of the phase diagram is shown in Fig. 5.

The standard deviation of the calculated data was $\sigma = 1.14\,°C$. The coordinates of eutectic point are 11.5 mol% $La_2O_3$ and 934 °C.

From the very similar behaviour of the systems $Na_3AlF_6$–$La_2O_3$ and $K_3AlF_6$–$La_2O_3$ one may conclude that the similar reaction takes part in the system
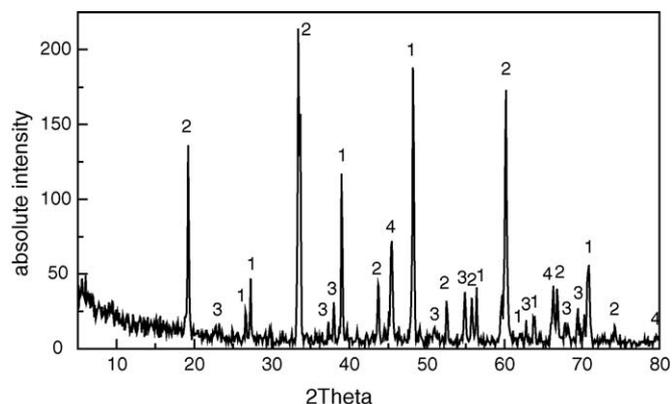
$$K_3AlF_6 + La_2O_3 \rightarrow 2KF + KLaF_4 + LaAlO_3$$



Fig. 4. X-ray record of the frozen melt of the system $Na_3AlF_6$–$La_2O_3$ (10 mol% of $La_2O_3$). (1) $LaAlO_3$; (2) $NaLaF_4$; (3) $Na_3AlF_6$; (4) NaF.
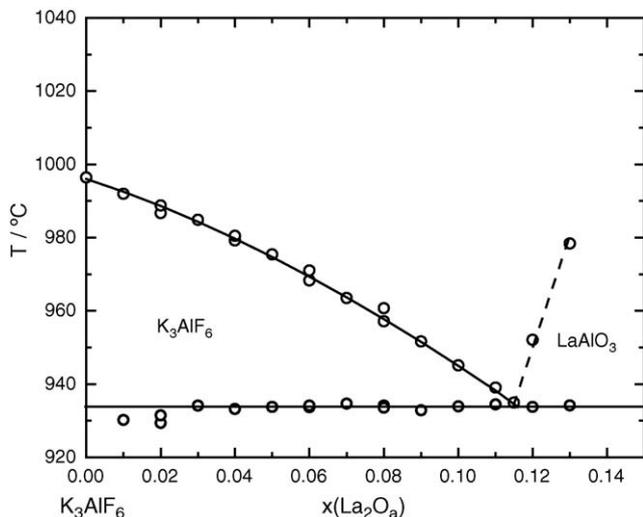
Fig. 5. Phase diagram of the system $K_3AlF_6$–$La_2O_3$. (◯) Experimental; (—) calculated.

Then probably $LaAlO_3$ is the first crystallizing phase at the measured compositions of the system higher than eutectic composition.

## 5. Conclusion

Solubility of lanthanum oxide in alkali cryolites is rather high. It suggests that chemical reactions between lanthanum oxide and cryolites take part in the systems. While in the system $Li_3AlF_6$–$La_2O_3$ alumina precipitates, in the other systems the mixed oxide $LaAlO_3$ is formed.

## Acknowledgment

## References

[1] Kirk-Othmer, Encyklopedia of Chemical Technology, vol. 17, fourth ed., John Wiley & Sons Inc., 1998.
[2] V. Šebian, V. Nečas, P. Dařílek, J. Electr. Eng. 52 (910) (2001) 299.
[3] I. Koštenská, M. Malinovský, Chem. Zvesti 36 (1982) 159.
[4] B. Gilbert, E. Robert, E. Tixhon, J.E. Olsen, T. Østvold, Inorg. Chem. 35 (1996) 4198.
[5] V. Danielik, J. Gabčová, P. Fellner, Chem. Pap. 53 (4) (1999) 233–237.
[6] V. Danielik, J. Gabčová, Thermochim. Acta 366 (2001) 79–87.
[7] V. Danielik, Chem. Pap. 59 (2) (2005) 81–84.
[8] V. Danielik, Ph.D. Thesis, STU Bratislava, 1997.
[9] V. Danielik, P. Fellner, Chem. Pap. 52 (4) (1998) 195–198.
[10] P. Fellner, V. Danielik, J. Thonstad, J. Appl. Electrochem. 30 (2000) 925–928.
[11] J. Thonstad, S. Rolseth, J. Rodseth, O. Lund, J. Tonheim, V. Danielik, P. Fellner, J. Híveš, Light Met. (2001) 441.